Environ Monit Assess (2017) 189: 74
DOI 10.1007/s10661-017-5792-y

Assessing the effects of dam building on land degradation in central Iran with Landsat LST and LULC time series

Reza Jafari · Seyedehnegar Hasheminasab

Received: 15 August 2016 / Accepted: 16 January 2017 / Published online: 24 January 2017

Abstract This study aimed to analyze the impact of Zayandehrood Dam on desertification using the spatio-temporal dynamics of land use/land cover (LULC) and land surface temperature (LST) in an arid environment in central Iran from 1987 to 2014. The LULC and LST images were calculated from Landsat TM, ETM+, and OLI data, and their accuracies were assessed against reference data using error matrix and linear regression analysis. Results showed that salty and bare lands increased up to 57,302 ha, while agricultural lands declined substantially (28,275.58 ha) in the region. The changes in LULC classes resulted in dramatic variations in LST values. The average temperature showed a 5.03 °C increase, and the minimum temperature increased by 5.66 °C. LST had an increasing trend in bare lands (8.74 °C), poor rangelands (6.8 °C), agricultural lands (9.46 °C), salty lands (9.6 °C), and residential areas (3.18 °C) in this 27-year period. Rainfall and temperature trend analysis revealed that the main cause of these extreme changes in LULC and LST was largely attributed to the drying up of Zayandehrood River due to dam construction and allocating water mainly for industrial sectors. Results indicate that in addition to LULC changes, the spatio-temporal variations of LST can be used as an effective index in desertification assessment and monitoring in arid environments.

R. Jafari (✉) · S. Hasheminasab
Department of Natural Resources, Isfahan University of Technology, Isfahan 841568311, Iran
e-mail: reza.jafari@cc.iut.ac.ir

Keywords Land degradation · Dam building · Zayandehrood Dam · LULC · LST

Introduction

Desertification is a major cause of many environmental, economic, and social problems in the world (Gonzalez 2001; Requier Desjardins et al. 2011; Bisaro et al. 2014). It is defined by the United Nation Convention to Combat Desertification (UNCCD) as "land degradation in arid, semi-arid and dry sub-humid areas resulting from various factors, including climatic variations and human activities". Desertification is not limited to drylands because loss of land productivity can result in the movement of the people from drylands to non-dryland areas; therefore, it is an issue of worldwide concern (Barbero-Sierra et al. 2015; Escadafal et al. 2015; Jafari and Bakhshandehmehr 2013; Miao et al. 2015; Torres et al. 2015; Vieira et al. 2015).

The amount of vegetation cover as well as its position in the landscape plays a major role in trapping resources (water, soil particles, and nutrients) and determining the landscape function. In fact, higher amount of vegetation within a particular landscape would prevent the leakage of resources. This positive influence of vegetation cover and other natural and organic mulches (e.g., crop residues and leaf litter) in soil erosion control and runoff reduction has been confirmed in many previous studies (Cerdà 1998; Moreno-Ramón et al. 2014; Sadeghi et al. 2015; Lieskovský and Kenderessy 2014; Cerdà et al. 2015). Unfortunately, vegetation degradation is one of

the main desertification processes in many drylands (Bastin et al. 1993; Dregne 2002; Ravi et al. 2010). It often occurs in rangelands and agricultural areas and starts with the reduction of vegetation cover. This can result from single or combined effects of mismanagement and drought. The effects of these are the appearance of barren soils and an increase in water losses and erosion rates which consequently can lead to ecosystem degradation (Plesník 2011; Berendse et al. 2015; Mekonnen et al. 2015; Zhao et al. 2013; König et al. 2014). Therefore, vegetation cover and consequently its variations in space and time are often used as one of the best indicators to assess and monitor desertification (Grunblatt et al. 1992; Becerril-Piña et al. 2015). The normalized difference vegetation index (NDVI) derived from satellite data has been widely used to estimate vegetation cover (Deering et al. 1975; Jury et al. 1997; Myneni et al. 1997; Prince 1991; Bannari et al. 1995; Tucker et al. 1991a; Vandandorj et al. 2015), and its capability has been shown in different desertification studies (Diouf and Lambin 2001; Nicholson et al. 1998; Prince and Justice 1991; Prince et al. 1998; Tucker et al. 1991b; Zhang et al. 2014). Land use and land cover (LULC) change due to human activities is another important indicator of desertification (Drake and Vafeidis 2004; Badreldin et al. 2014; Coppin et al. 2004). In addition to image-based vegetation and LULC indicators, land surface temperature (LST) can also be used as an effective indicator in desertification assessment and monitoring. LST is highly related to the dynamic of land surface processes (Dash et al. 2002; Serafini 1987; Price 1990); hence, its temporal and spatial variability is a good indicator of soil and vegetation conditions (Amiri et al. 2009; Zhang et al. 2010; Higuchi et al. 2007; Ghobadi et al. 2015). One of the main characteristics of vegetation cover in arid environments is its sparseness; consequently, soil is the dominant land surface component in these regions. It is well known that estimating vegetation cover from NDVI and classification techniques is often influenced by soil background effects (Huete et al. 1985; Smith et al. 1990). The LST indicator appears to be less sensitive to soil-vegetation interactions, and this can be an important advantage for remote sensing of land conditions in arid and semi-arid regions; therefore, further research is recommended in this field.

Drylands cover more than 85% of Iran and are very prone to desertification (Le Houérou 1992). Iran includes 31 provinces with a land area of about 1.64 million km^2 and annual temperature ranging from −20 to +40 °C. The amount of annual precipitation is approximately 1200 mm in the north and less than 100 mm in the central regions (Amiraslani and Dragovich 2011). According to land use/cover map of Iran, deserts, rangelands, agricultural lands, forests, and residential areas cover 20, 55, 11, 8, and 6%, respectively (FRW 2005). Due to Iran's climate and topographic conditions, 75 and 20 million ha are affected by water and wind erosion, respectively (Asadi et al. 2012), and the average national rate of water erosion has been reported from 15 to 45 Mg ha^{-1} $year^{-1}$(Amiraslani and Dragovich 2011). According to the Bureau of Desert Affairs of Iran, 17 provinces have desert areas which are home to approximately 70% of the total population of the country, and about 20% of these regions has been effected by desertification processes. The main causes of desertification in Iran are water resource depletion, population pressure, excessive grazing, wrong management practices, and climatic factors (Ghaffari et al. 2010). Iran, as a member of UNCCD, has executed many projects to combat desertification (Amiraslani and Dragovich 2011), it seems these activities in comparison with the rate of degradation in the country are not adequate. For example, a study by Jafari and Bakhshandehmehr (2013) in central Iran showed that 9.49% (1.01 million ha) of the region has been affected by low desertification, 56.4% (6.04 million ha) by moderate, 31.74% (3.4 million ha) by severe, and 2.33% (0.25 million ha) by very severe.

Dam building is another major human activity which has accelerated desertification in Iran (Zafarnejad 2009). Although supply of water for irrigation, domestic needs, power generation, flood control, navigation, and recreational opportunities are the main positive effects of dam building, its environmental and social consequences should also be considered. Important examples include landscape structure change (Cooper et al. 2015), fragmenting and transforming water flows (Fearnside 2016), loss of species diversity (Palmeirim et al. 2014), the spread of invasive species (Kellogg and Zhou 2014), ecosystem loss (Bauni et al. 2015; Fan et al. 2015; Palmeirim et al. 2014), greenhouse gas emission (Fearnside and Pueyo 2012), drying up of wetlands (Lyon and Greene 1992; Micklin 2007), submergence of valleys and low lying sites, and social impacts (Fearnside 2016; De Pina Tavares et al. 2014). A lot of studies, such as the ones mentioned above, on the impacts of dams on the ecosystems and human lives

can be found in the literature, but their negative effects on land degradation in arid and semi-arid regions have seldom been discussed in detail. Currently, 647 dams are in operation in Iran, 146 are being built, and 537 are being designed by governmental and non-governmental organizations (WRM 2015). Because of the lack of data about the effects of dam building on desertification process and also the broad extent of the areas affected by desertification, remotely sensed derived LULC and LST could be used as appropriate indicators of desertification. No research so far has evaluated the relationship between satellite-based indicators of LULC and LST in desertification assessment and monitoring. Neither has any work examined the usefulness of LST trend as an indicator of desertification. Therefore, this study aimed to analyze the impact of Zayandehrood Dam on desertification using the spatio-temporal dynamics of LULC and LST in an arid environment in central Iran from 1987 to 2014. The specific objectives of this study were (i) to map and monitor the spatio-temporal changes of LULC and LST using Landsat satellite data for years 1987, 1998, 2001, 2002, 2009, 2010, 2011, and 2014; and (ii) to investigate the trend of desertification process based on the LULC and LST indicators in the region.

Materials and methods

Study area

The study area with 347,400.8 ha located in the eastern part of Isfahan province and lies between latitudes 32° 24″ N and 32° 44″ N and longitudes 51° 39″ E to 52° 56″ E (Fig. 1). The climate in the study area is characterized by hot summers and cold winters. The mean daily maximum temperature ranges from 43.5 °C in summer to approximately 27.4 °C in winter, and mean daily minimum temperature ranges from 5.8 °C in summer to about −25.9 °C in winter. The mean annual evaporation rate is approximately 3200 mm, and prevailing winds are from the southeast. Rainfall is highly variable from year to year, and long-term average of annual rainfall is 104.26 mm (SD = 34.6). Rainfall and air temperature data of East Isfahan station from 1976 to 2014 and Daran station from 1992 to 2014 were used to detect trends in climate parameters (annual rainfall, mean annual temperature, mean annual maximum and minimum temperatures) in the region (Fig. 2). Isfahan province is surrounded by Dasht-e Kavir desert in the East and North and the Zagros Mountains in the West and South. The Zagros Mountains produce a foehn effect that reduce the rainfall in the Isfahan region and then cause desert-like conditions. The water resources of the Isfahan province are coming from rivers (e.g., Zayandehrood), springs, wells, and qanats. Zayandehrood is the largest river in the central plateau of Iran. It begins in the Zagros Mountains and flows 400 km eastward before ending in the Gavkhouni international wetland, southeastern of Isfahan city. The Zayandehrood Dam was constructed on this river in 1970 for reducing floods, producing hydroelectricity, and also for agricultural, domestic, and industrial needs (Fig. 3).

Landsat satellite imagery

Multispectral Landsat satellite imagery is one of the most widely used forms of remote sensing data for many environmental applications. The availability of extensive archives of Landsat makes it suitable for many environmental management programs. We used eight sub-scenes of Landsat imagery (Table 1) to investigate the effects of LULC changes on the dynamics of LST. To minimize the effects of seasonal and phonological changes and also exclude cloud cover, the images were acquired almost in the same time (late May in spring season) based on available data. All the Landsat images were geometrically corrected to the Universal Transverse Mercator (UTM, Zone 39N) coordinate system using a 1:25,000 topographic map. A minimum of 15 ground control points (GCPs) were selected throughout the topographic map and raw image (ETM+ panchromatic band). The raw image was transformed to the reference map using a first order polynomial and then resampled using the nearest neighbor method. The root–mean-square error (RMSe) of the transformation was about 0.46 pixel indicating that the image geometric correction was accurate within one pixel. The same method was used to register the remaining images to the ETM+ panchromatic band using image-to-image registration.

Image processing

Maximum likelihood classifier, as one of the most common image classification technique, was chosen

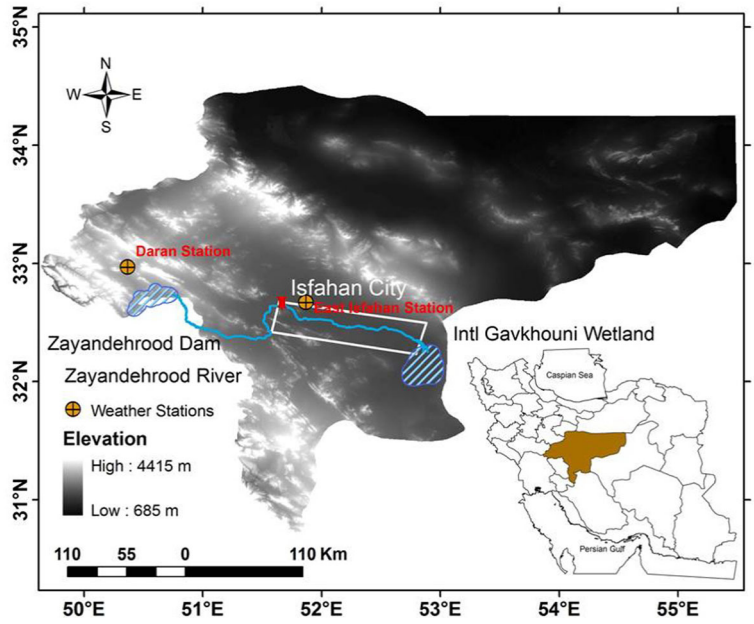

Fig. 1 Location of study area in Isfahan province and Iran. Shown also are Isfahan City and the Daran and East Isfahan weather stations

to classify Landsat images from May 1987 to May 2014. After classification process, to assess the accuracy of the classified images, the overall accuracy and kappa statistics were calculated based on the error matrix. A stratified random sampling was used to collect reference data for accuracy assessment. Reference data were obtained by using FCC images, 1:50,000 and 1:25,000 topographic maps, and GPS points collected during field works. The result of the accuracy assessment for each classified image was an error matrix showing overall accuracy, error of omission, producer's accuracy, error of commission, user's accuracy, and a kappa coefficient (Lillesand and Kiefer 2000). After accuracy assessment, the post-classification technique was used to compare classified images for determining LULC changes over 27 years.

To investigate temporal dynamics of mean LST in each LULC class, LST was calculated using thermal bands of Landsat 5, 7, and 8 (10.40–12.50 μm) as follows. First, the digital number (DN) values of Landsat 5 and 7 were converted to spectral radiance based on the sensor's reference values (Amiri et al. 2009):

$$L_\lambda = [(L_{\max} - L_{\min})/(\mathrm{QCal}_{\max} - \mathrm{QCal}_{\min}) \times \mathrm{QCal}] + L_{\min} \quad (1)$$

where $QCal_{\min} = 1$, $QCal_{\max} = 255$, $QCal = \mathrm{DN}$, $L_{\max}$, $L_{\min}$ = spectral radiance for band 6 at DN 255 and 1,

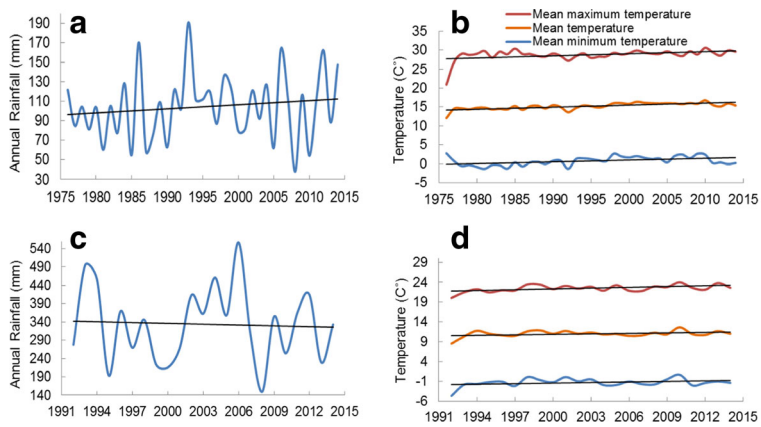

Fig. 2 Annual rainfall, temperature fluctuations, and straight-line trends in the studied years. **a**, **b** East Isfahan station. **c**, **d** Daran station

Fig. 3 Zayandehrood Dam and its effect on desertification. Photographs of **a** Zayandehrood dam, **b** Zayandehrood River, **c** abandoned agricultural land, and **d** salinized agricultural land

respectively (Wm^{-2} sr^{-1} μm^{-1}). For Landsat 8, the following equation was used to transform DN values to spectral radiance (USGS 2013).

$$L_\lambda = M_L QCal + A_L \quad (2)$$

where M_L = band-specific multiplicative rescaling factor from the metadata and A_L = band-specific additive rescaling factor from the metadata. Second, the spectral radiance was transformed to blackbody temperature by using following equation:

$$T_b = K_2 / Ln((K_1/L_\lambda) + 1) \quad (3)$$

where T_b = effective at-satellite temperature K, K_1 = first calibration constant (W m^{-2} sr^{-1}) = 666.09, K_2 = second calibration constant (K) = 1282.7, and L_λ = spectral radiance (W m^{-2} sr^{-1} μm^{-1}). Then, land surface temperature was calculated for each image and was converted to Celsius units (Eq. 4) (Artis and Carnahan 1982):

$$T_s = T_b / [1 + (\lambda T_b / \alpha) Ln\varepsilon] \quad (4)$$

where λ = wavelength of radiance and $a = hc/k$ (h = Planck's constant; c = velocity of light) (k = Boltzmann

Table 1 Details information of the Landsat satellite images

Satellite	Sensor	Acquisition	WRS[1] (Pass/row)	Spatial resolution (m)	No. of bands
Landsat 5	TM	1987/05/29	163/38	30, 120	7
Landsat 5	TM	1998/06/12	163/38	30, 120	7
Landsat 7	ETM+	2001/05/27	163/38	15, 30, 60	8
Landsat 7	ETM+	2002/05/14	163/38	15, 30, 60	8
Landsat 5	TM	2009/05/25	163/38	30, 120	7
Landsat 5	TM	2010/05/28	163/38	30, 120	7
Landsat 5	TM	2011/05/31	163/38	30, 120	7
Landsat 8	OLI	2014/05/23	163/38	15, 30, 100	11

[1] World Wide Reference System

constant). The emissivity (ε) was calculated by using NDVI index based on red and near-infrared (NIR) bands of Landsat TM, ETM+, and OLI sensors (Eq. 5). On the basis of NDVI values, the emissivity images for each date were produced (Momeni and Saradjian 2008; Liu and Zhang 2011) (Table 2).

$$\mathrm{NDVI} = (NIR - RED)/(NIR + RED) \quad (5)$$

Among the extracted LST images, the 2014 one was selected for accuracy assessment purposes. Ground LST data from 15 GPS sample sites were collected using digital thermometer on 23rd of May 2014. Sample sites were chosen to include different LULC classes. In order to evaluate whether the LST images could be used to predict field LST data, linear regressions were used to examine their relationships as well as trends in climate parameters. Image LST data were extracted using a 180-m buffer around sample sites.

Results and discussion

LULC maps

The LULC maps were produced from the maximum likelihood classification method for eight Landsat images (Fig. 4). The figure shows that TM 1987, TM 1998, ETM+ 2001, ETM+ 2002, TM 2009, TM 2010, TM 2011, and OLI 2014 images were classified into eight classes including bare land, poor rangeland, agricultural land, salty land, water (Zayandehrood River), residential area, sand dune, and non-vegetated hill. Agricultural and bare land classes have changed the most between different years of the study. The agricultural lands which are located along the Zayandehrood River and stretched from Isfahan city to Gavkhouni international wetland in the eastern parts of the study area showed a 48.33% (28,275.58 ha) reduction from 1987 to 2014. A decreasing trend in this land use is evident in Figs. 4 and 5, although it increased in 1998 and 2002 due to higher rainfall and also Zayandehrood Dam shutter opening in 2010 (Nourian 2014). The bare land class, on the other hand, showed a 30.65% (46,654.7 ha) increase which indicates the severity of desertification crisis in this arid environment. The sand dunes and non-vegetated hills remained almost constant, but the rangeland and salty land had medium changes in comparison to the agricultural and bare land ones. The water (Zayandehrood River) and residential area classes also showed considerable changes during the study period.

The overall classification accuracy for all the maps was higher than 82% (Table 3). The overall accuracy and overall kappa coefficients of the classification ranged from 82 to 92% and from 77 to 90%, respectively. These results generally suggest that there is a good agreement between the LULC maps and actual LULC categories on the ground (Landis and Koch 1977; Torres-Vera et al. 2009; Amuti and Luo 2014). In terms of producer's and user's accuracy, classes ranged from 20.7 to 99.5%. Among the classes, the non-vegetated hill had the lowest accuracy (20.7%) due to its spectral similarity to bare land and poor rangeland. Results also showed that the closeness of classified maps to the reference data affects the accuracy of the classification. For example, because of the closeness of 2014 LULC map to the reference data taken from GPS, receiver showed higher accuracy. Whereas, due to the time difference between the 1987 LULC and 1976 topographic map, the overall accuracy was less than other classified maps in the study area (Kiage et al. 2007).

The performance of change detection methods varies due to topographic conditions, vegetation composition and phenology, and background soil effects. A number

Table 2 Emissivity values based on NDVI data

NDVI values	Emissivity (ε)	Land surface feature
NDVI < −0.185	0.99	Water
−0.185 ≤ NDVI < 0.156	0.9636 + 0.00612 × NDVI	Soil and very poor vegetation
0.156 ≤ NDVI ≤ 0.46	0.9740 + 0.0036 × Pv (vegetation fraction) $Pv = (NDVI - NDVI_{min})^2/(NDVI_{max} - NDVI_{min})^2$	Medium vegetation
NDVI > 0.46	0.987	Dense vegetation

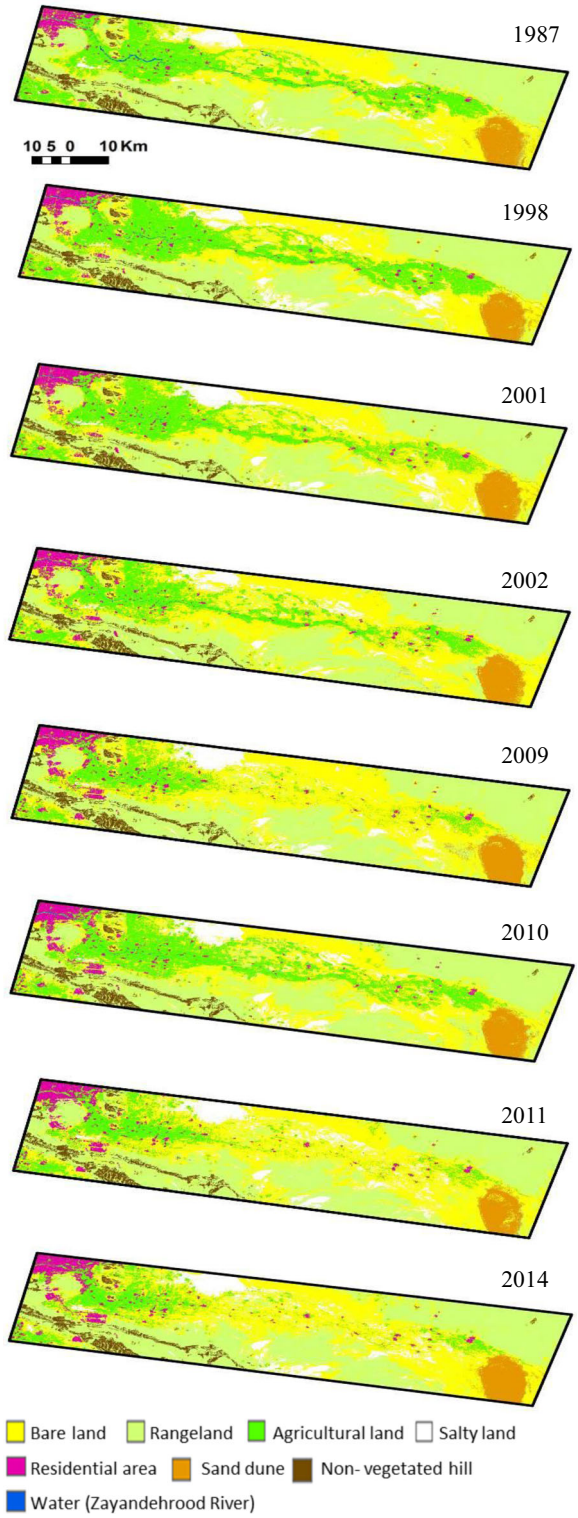

Fig. 4 LULC maps produced from the maximum likelihood classifier from 1987 to 2014

of studies have shown that the post-classification method reduces the impact of atmospheric and environmental differences and provides a complete matrix of change directions (Mas 1999; Mundia and Aniya 2006; Singh 1989). Therefore, this method was used for change detection purposes from 1987 to 2014. As it can be seen from Fig. 5, bare land class included around 30.38% of the area (105,556 ha) in 1987, while in 2014, it increased to 43.81%. In other words, about 46,654.7 ha has been degraded in this period. Human impacts such as Zayandehrood Dam construction and population increase in the region appear to be the main reasons for these dramatic changes. Although dams have important roles in utilizing water resources and storing water for times of need, it is very important to reduce their negative effects on environment. In the study area, about 5400 ha of rangelands were inundated due to dam construction. A study in Australia also showed that the construction of a reservoir in Victoria has inundated 1925 ha of land and has caused considerable LULC change in the region (Wijesundara and Dayawansa 2011). Rautela et al. (2002) reported that the construction of Tehri Dam in India has caused approximately 6000 ha change in LULC over 10 years. Some studies in Iran have also shown that dams (e.g., Taleghan and Sattarkhan dams) have had a major role in LULC changes, and most of the natural ecosystems are under threat due to the activities in upland/lowland regions of dams (Farajzadeh and Rostamzadeh 2007; Matkan et al. 2010). To date, there have been no studies in Iran that have evaluated the impacts of dams on plant and animal diversity before and after dam construction, and this can be an important direction for future work. According to Fig. 5, 25% of poor rangeland class (34,557.3 ha) has been degraded and salty lands showed an increase of 37.5% (10,647.4 ha) between 1987 and 2014. The residential areas increased consistently over the 27 years of the study. These areas in 2014 were 1.8 times greater than the year 1987. The area of water class (Zayandehrood River) was about 1378.08 ha in 1987 and 233.38 ha in 2014 which indicates around 83% reduction in the surface water of the region.

The dynamics of LST

Figure 6 shows the spatio-temporal distribution of LST in the region from 1987 to 2014. High temperatures mostly occurred in the eastern parts of the region, and the temperature increased from west to east. Very high

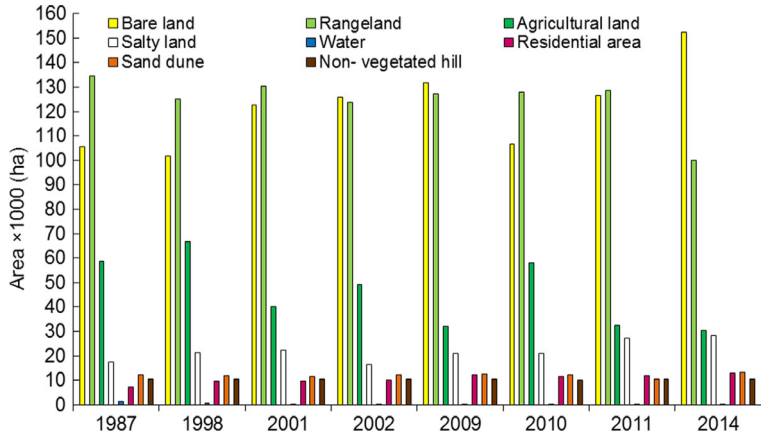

Fig. 5 Area of different LULC classes from 1987 to 2014

increase in LST values was observed in the central parts of the LST images year by year. The main reason for this increase was the vegetation degradation because of decreasing surface water in the Zayandehrood River. The average temperature showed a 5.03 °C increase and the minimum temperature increased 5.66 °C during this period. The average LST ranged from 24.31 °C in the Zayandehrood River bed in 1987 to 48.12 °C in sand dune class in 2014. The average temperatures were 37.38 and 42.42 °C in 1987 and 2014, respectively (Table 4).

The high relationship between 2014 LST image and LST field data showed that satellite data can be used to predict ground surface temperature in the region. The LST was correlated significantly with LST ground data ($p < 0.05$), explaining up to 80% of the variation in field measurements (Fig. 7). In considering predictive relationships between image LST and the field measurements at the sample sites, it must be remembered that the LST data was collected over few hours, and that the imagery has captured landscape conditions at one time during this period. Consequently, temporal variation in ground LST must be considered as a contributor to variability in the field data. In addition, slight mismatch between the precise area sampled in the field and the pixels extracted from the imagery could also potentially reduce the strength of relationships between the two data sets.

Table 3 Overall accuracy and kappa coefficients of the classified satellite images in different years

Satellite sensor	Acquisition date	Overall accuracy (%)	Overall kappa coefficients (%)
TM	1987	83.4	77.08
TM	1998	82.1	79.48
ETM+	2001	86.5	81.25
ETM+	2002	88.4	80.65
TM	2009	89.9	84.26
TM	2010	88.5	86.76
TM	2011	91.8	87.39
OLI	2014	92	90.68

The trend of LST changes for each LULC type from 1987 to 2014 is shown in Fig. 8. Among the LULC classes, sand dunes had the highest average temperature, followed by bare land and poor rangeland, non-vegetated hill, salty land, residential area, agricultural land, and water (Zayandehrood River). The average LSTs for water, sand dunes, and non-vegetated hills were 28.72, 47.55, and 43.92 °C. They had almost constant trend from 1987 to 2014, although the water class showed the lowest temperature (24.31 °C) due to the large amount of water flowing in the Zayandehrood River in 1987. The average LST changes in the salty lands and residential areas were minor from 1987 to 2009, but increased by 4 and 2.46 °C between 2009 and 2014, respectively. The temperature trend of poor rangeland was almost similar to bare land class. LST was 40.62, 40.87, and 41.48 °C in 1987, 2002, and 2009, but increased to 45.93 °C in 1998, 49.92 °C in 2010, 47.56 °C in 2011, and 47.42 °C in 2014, respectively. The LST of agricultural land changed significantly in this 27-year period. The mean LST was 27.61 °C in 1987 but increased by 2.52, 5.28, 3.58, 3.74, 6.57, 7.37,

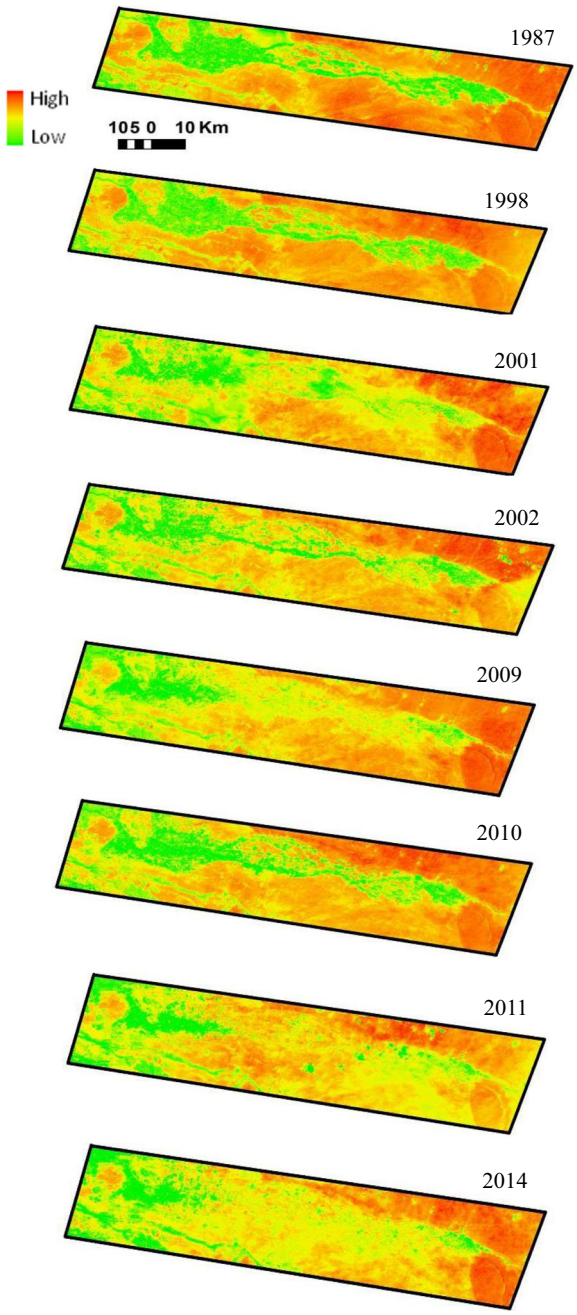

Fig. 6 The spatio-temporal distribution of LST from 1987 to 2014

and 9.46 °C in 1998, 2001, 2002, 2009, 2010, 2011, and 2014, respectively. The positive trend of LST in most of the years in this land use appears to be the result of water shortage, plant water stress, and increasing sparse vegetation cover and background soil. The bare land class also had an increasing trend from 1987 to 2014, although its temperature decreased to 39.26 °C in 2002.

Relationships of LULC and LST changes with desertification

The study area has experienced significant changes in LULC and LST from 1987 to 2014. The main cause of these changes is water shortage as a result of water resources mismanagement in the region. Until the 1960s, most of the water in the Zayandehrood River has been used in the agriculture sector. With growing population and the creation of large steel works and other industries, the pressure on water resources steadily increased. Therefore, the Zayandehrood Dam was constructed in 1970 and around 80% of its water was allocated for agriculture, 10% for human consumption, 7% for industry (e.g., Zobahan-e-Esfahan and Foolad Mobarekeh steel companies, Isfahan's petrochemical, refinery, and power plants), and 3% for other uses (Gandomkar and Fouladi 2012). Over the past years, drought conditions in the region (Molle and Mamanpoush 2002; Nourian 2014; NDWMC 2015) and also allocating water mainly for industrial sectors in the upper areas of the Zayandehrood basin have caused the river to dry out completely in most of the years. As a result, a large amount of agricultural lands in the study area which critically depended on the supply of the dam have been converted to desertified areas. Other studies have also shown that dam construction and diversion of upstream water for industry and other uses are the main causes of desertification (Ebrahimzadel 2009; Najafi and Vatanfada 2011; Indoitu et al. 2015).

The changes in LULC resulted in changes in LST, especially in the agricultural and bare lands. As it can be seen from Fig. 8, there is a sharp increase in the LST values in all classes except sand dunes and non-vegetated hills from 2009 to 2014. It is clear that the spatial distribution of natural vegetation cover and its condition strongly depends on climate parameters such as rainfall. The rainfall ranged from 38.1 in 2008 to 190.8 mm in 1993 in the study area. As it can be seen from Fig. 8, rangeland vegetation cover and consequently rangeland condition has been influenced by the rainfall. For example, the year 2009 (117 mm) and also 2002 (121 mm) with high rainfall had lower temperature, and the year 2010 with the lowest rainfall (54 mm) in the studied period had the highest LST. The increased temperature (2.75 °C) in the residential areas was due to urban expansion during the 27-year period. For

Table 4 Minimum, maximum, and average LST from 1987 to 2014

Year	LST (°C)			Year	LST (°C)		
	Minimum	Maximum	Average		Maximum	Minimum	Average
1987	17.36	49.15	37.38	2009	49.50	22.84	39.35
1998	20.42	54.87	39.92	2010	51.58	19.17	42.72
2001	21.90	51.30	39.54	2011	53.95	24.40	42.22
2002	18.31	51.63	38.78	2014	53.08	23.02	42.42

example, residential areas increased about 5814.12 ha between 1987 and 2014. The conversion of agricultural lands into residential areas has been another important factor for increasing temperature in this land use.

In order to examine the effects of dam building and climate change on temperature increase in the study area, temperature variables including annual mean temperature and annual mean maximum and minimum temperatures were analyzed for the East Isfahan station. All the variables had significant relationships with the studied years in this station. These variables showed an increasing trend of 0.055 °C year^{-1}(statistically significant at $p < 0.001$), 0.052 °C year^{-1} (statistically significant at $p < 0.05$), and 0.046 °C year^{-1}(statistically significant at $p < 0.001$), respectively. Several studies have also reported that climate change has occurred, and temperature has increased in different parts of the country (Ahmadi et al. 2015; Ataei and Fanaei 2014; Deenpajouh et al. 2013; Sabzalipour et al. 2013; Behmanesh and Azadetalatappeh 2013). The regression analysis of rainfall data for the East Isfahan station showed no significant difference in the mean of annual rainfall over the period of 35 years ($p > 0.39$), although rainfall had an increasing trend of 0.43 mm year^{-1}(e.g., Modarres et al. 2007; Khodagholi et al. 2014). The rainfall and temperature variables of Daran station which is located outside the study area and upstream of the Zayandehrood dam were compared with the East Isfahan station to see whether the effect of climate change can be separated from dam building. Similar to the East Isfahan station, there was no significant difference in the mean of annual rainfall from 1992 to 2014 ($p > 0.829$) and rainfall had a decreasing trend of −0.72 mm year^{-1}. The annual mean temperature and annual mean maximum and minimum temperature variables showed an increasing trend of 0.036, 0.067, and 0.044 °C year^{-1}, respectively. Among the variables, only the annual mean maximum temperature had significant relationship with the years at the 95% confidence level. The increasing trend of temperature at both stations indicated that global warming has occurred in the region. However, there were stronger relationships between all the temperature variables and the studied years at the East Isfahan station. In addition, the rates of temperature increase in the annual mean and minimum temperatures at the East Isfahan station was 0.019 and 0.002 °C year^{-1} higher than the Daran station, respectively. These increases in temperature at the East Isfahan station might have been as a result of increasing trend of LST due to dam building and increasing bare lands in the study area. Other studies (Salazar et al. 2015; Xiao and Weng 2007; Liu et al. 2014) have also shown that LULC changes play important role in surface temperature fluctuations.

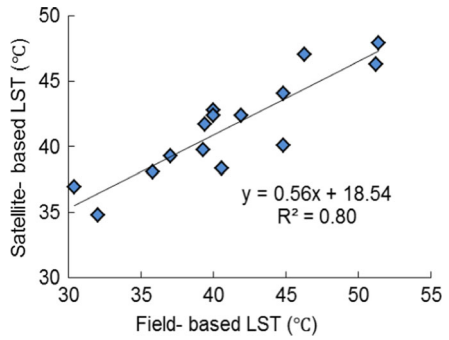

Fig. 7 Relationship between field and satellite LST data ($N = 15$) in 2014

Agriculture is the major land use in the study area and the people of the region totally depend on it for their livelihoods. Drying up of Zayandehrood River has had a major impact on the region's population lives and has raised many concerns such as immigration and poverty. On the other hand, because of the lack of surface water and low quality of

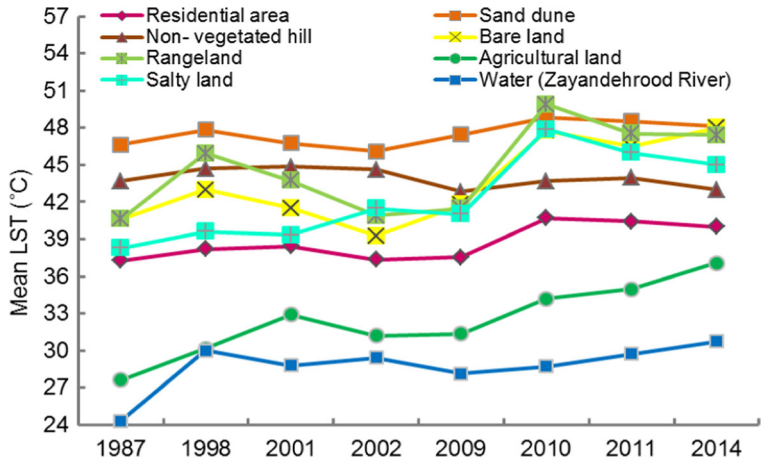

Fig. 8 The trend of mean LST in different LULC classes from 1987 to 2014

groundwater, salty lands have also increased about 10,647.3 ha during the study period which resulted in increasing LST around 6.71°C. Overall, the results showed that the area of vegetation and soil-related classes especially the agricultural and bare land ones have continuously decreased and increased in the region, respectively. For example, the bare lands have expanded an average about 5831.75 ha each year which indicates the high level of land degradation in this arid environment. Although Zayandehrood Dam provided adequate water for irrigation of the lands in the first few years of opening, the amount of water for agricultural purposes especially in the study area reduced year by year. The shortage of surface water in the region has degraded the quality of groundwater. According to Jafari and Bakhshandehmehr (2013), the amount of electrical conductivity (EC), chloride rate (Cl), sodium adsorption ratio (SAR), and total dissolved solids (TDS) indices were very high in terms of desertification, and the quality of groundwater decreases from west to east especially in the eastern parts of the region where the groundwater level is shallow and non-clastic minerals are dominated. In addition to low quality of ground water, using flood irrigation which is one of the most common techniques in the region in which 70% of water is lost through evaporation (Karimkoshteh and Haghiri 2004) has increased soil degradation and desert-like conditions (Xie et al. 2015). Due to lack of surface water and over-exploitation of underground water for agricultural purposes, a major decline in water table of the study area has occurred and caused an increase in land subsidence. For example, there is an annual decline of 50 cm in the level of water table of the region.

Conclusions

Although dams have important roles in utilizing water resources and development programs, their negative effects on the environment must also be considered. This study has examined the spatio-temporal dynamics of land use/land cover (LULC) and land surface temperature (LST) as indicators of desertification in an arid environment in central Iran resulting from Zayandehrood Dam construction. The results showed that salty and bare lands increased, while agricultural lands declined substantially from 1987 to 2014. The main causes of agriculture decline were largely attributed to the drying up of Zayandehrood River due to the dam construction and allocating water mainly for industrial sectors. Changes in the agricultural lands and also other LULC classes were also observed in the LST outputs. Increasing trend in the mean of temperature was observed in all LULC classes except in sand dunes and non-vegetated hills. The integration of LULC and LST indicators revealed that the study area has experienced significant desertification over the 27-year period. If the current scenario of degradation continues, the study area which is a part of marginal lands of Gavekhouni international wetland could be an important dust source at regional, national, and international scales in the near future. The results of this study showed that, in addition to LULC changes, increasing trend

in LST can be used as an effective index for desertification assessment and monitoring in arid environments. This finding indicates that the LST satellite-based indicator has high capability for distinguishing the areas affected by desertification and may be used for reporting the condition of desertification at national scale. Therefore, our recommendation is that the performance of this indicator in desertification mapping must be further examined in other regions with the similar characteristics. Further work is also needed to investigate the spatio-temporal variations of LST resulting from seasonal changes.

References

Ahmadi, M., Lashkari, H., Keikhosravi, Q., & Azadi, M. (2015). Analysing the threshold temperature indices in detecting climate change in Great Khorasan. *Geography, 45*, 53–75.

Amiraslani, F., & Dragovich, D. (2011). Combating desertification in Iran over the last 50 years: an overview of changing approaches. *Journal of Environmental Management, 92*(1), 1–13.

Amiri, R., Weng, A., Mohammadi, A., & Alavipanah, S. K. (2009). Spatial-temporal dynamics of land surface temperature in relation to fractional vegetation cover and land use/cover in the Tabriz urban area, Iran. *Remote Sensing of Environment, 113*, 2606–2617.

Amuti, T., & Luo, G. (2014). Analysis of land cover change and its driving forces in a desert oasis landscape of Xinjiang, northwest China. *Solid Earth, 5*(2), 1071–1085.

Artis, D. A., & Carnahan, W. H. (1982). Survey of emissivity variability in thermography of urban areas. *Remote Sensing of Environment, 12*, 313–329.

Asadi, H., Raeisvandi, A., Rabiei, B., & Ghadiri, H. (2012). Effect of land use and topography on soil properties and agronomic productivity on calcareous soils of a semiarid region, Iran. *Land Degradation & Development, 23*(5), 496–504.

Ataei, H., & Fanaei, R. (2014). Detecting the trend of daily mean temperature in Isfahan province in the last 50 years. *Geography and Environmental Planning, 25*, 105–118.

Badreldin, N., Frankl, A., & Goossens, R. (2014). Assessing the spatiotemporal dynamics of vegetation cover as an indicator of desertification in Egypt using multi-temporal MODIS satellite images. *Arabian Journal of Geosciences, 7*(11), 4461–4475.

Bannari, A., Morin, D., & Bonn, F. (1995). A review of vegetation indices. *Remote Sensing Review, 13*, 95–120.

Barbero-Sierra, C., Marques, M. J., Ruiz-Pérez, M., Escadafal, R., & Exbrayat, W. (2015). How is desertification research addressed in Spain? Land versus soil approaches. *Land Degradation & Development, 26*(5), 423–432.

Bastin, G. N., Pickup, G., Chewings, V. H., & Pearce, G. (1993). Land degradation assessment in central Australia using a grazing gradient method. *Rangeland Journal, 15*, 190–216.

Bauni, V., Schivo, F., Capmourteres, V., & Homberg, M. (2015). Ecosystem loss assessment following hydroelectric dam flooding: the case of Yacyretá, Argentina. *Remote Sensing Applications: Society and Environment, 1*, 50–60.

Becerril-Piña, R., Mastachi-Loza, C. A., González-Sosa, E., Díaz-Delgado, C., & Bâ, K. M. (2015). Assessing desertification risk in the semi-arid highlands of central Mexico. *Journal of Arid Environments, 120*, 4–13.

Behmanesh, J., & Azadetalatappeh, N. (2013). Analysing the changes of effective parameters on Orumiyeh's climate. *Journal of Geography and Planning, 19*, 41–58.

Berendse, F., Van Ruijven, J., Jongejans, E., & Keesstra, S. D. (2015). Loss of plant species diversity reduces soil erosion resistance of embankments that are crucial for the safety of human societies in low-lying areas. *Ecosystems, 18*, 881–888.

Bisaro, A., Kirk, M., Zdruli, P., & Zimmermann, W. (2014). Global drivers setting desertification research priorities: insights from a stakeholder consultation forum. *Land Degradation & Development, 25*(1), 5–16.

Cerdà, A. (1998). The influence of aspect and vegetation on seasonal changes in erosion under rainfall simulation on a clay soil in Spain. *Canadian Journal of Soil Science, 78*(2), 321–330.

Cerdà, A., González-Pelayo, O., Giménez-Morera, A., Jordán, A., Pereira, P., Novara, A., et al. (2015). The use of barley straw residues to avoid high erosion and runoff rates on persimmon plantations in Eastern Spain under low frequency–high magnitude simulated rainfall events. *Soil Research, (In press)*.

Cooper, A. R., Infante, D. M., Wehrly, K. E., Wang, L., & Brenden, T. O. (2015). Identifying indicators and quantifying large-scale effects of dams on fishes. *Ecological Indicators, (In press)*.

Coppin, P., Jonckheere, I., Nackaerts, K., Muys, B., & Lambin, E. (2004). Digital change detection methods in ecosystem monitoring: a review. *International Journal of Remote Sensing, 25*(9), 1565–1596.

Dash, P., Tsche, F. M. G., Olesen, F. S., & Fischer, H. (2002). Land surface temperature and emissivity estimation from passive sensor data: theory and practice-current trends. *International Journal of Remote Sensing, 23*(13), 2563–2594.

De Pina Tavares, J., Ferreira, A. J. D., Reis, E. A., Baptista, I., Amoros, R., Costa, L., et al. (2014). Appraising and selecting strategies to combat and mitigate desertification based on stakeholder knowledge and global best practices in Cape Verde archipelago. *Land Degradation & Development, 25*(1), 45–57.

Deenpajouh, Y., Niyazi, F., & Mofeed, H. (2013). Trend of climate parameters in Tabriz. *Journal of Geography and Planning, 19*, 145–169.

Deering, D. W., Rouse, J. W., Hass, R. H., & Schell, J. A. (1975). Measuring forage production of grazing units from Landsat MSS data. In *Proceedings of the 10th International Symposium on remote sensing of environment*. 6–10 October, Ann Arbor, MI, pp. 1169–1178.

Diouf, A., & Lambin, E. (2001). Monitoring land-cover changes in semiarid regions: remote sensing data and field observations in the Ferlo, Senegal. *Journal of Arid Environments, 48*, 129–148.

Drake, N. A., & Vafeidis, A. (2004). A review of European Union funded research into the monitoring and mapping of

Mediterranean desertification. *Advances in Environmental Monitoring and Modelling, 1*(4), 1–15.

Dregne, H. E. (2002). Land degradation in the drylands. *Arid Land Research and Management, 16*, 99–139.

Ebrahimzadel, I. (2009). Analysis of the recent droughts and lack of water in Hamoon Lake on Sistan economic functions. *Iran-Water Resources Research Journal, 5*(2), 30–32.

Escadafal, R., Barbero-Sierra, C., Exbrayat, W., Marques, M. J., Akhtar-Schuster, M., El Haddadi, A., et al. (2015). First appraisal of the current structure of research on land and soil degradation as evidenced by bibliometric analysis of publications on desertification. *Land Degradation & Development, 26*(5), 413–422.

Fan, H., He, D., & Wang, H. (2015). Environmental consequences of damming the mainstream Lancang-Mekong River: a review. *Earth-Science Reviews, 146*, 77–91.

Farajzadeh, M., & Rostamzadeh, H. (2007). Evaluating the effect of large dams on land use changes using remote sensing and GIS. *Modares Human Sciences, 11*(1), 47–66.

Fearnside, P. (2016). Environmental and social impacts of hydroelectric dams in Brazilian Amazonia: implications for the aluminum industry. *World Development, 77*, 48–65.

Fearnside, P., & Pueyo, S. (2012). Greenhouse-gas emissions from tropical dams. *Nat. Climate Change, 2*, 382–384.

FRW (2005). Land cover map of Iran, Final Report, winter 2005, The Forest, Rangeland and Watershed Management Organization, Tehran, Iran.

Gandomkar, A., & Fouladi, K. (2012). The necessity of optimized management on surface water sources of Zayanderood basin. *World Academy of Science, Engineering and Technology, 6*(5), 468–472.

Ghaffari, G., Keesstra, S., Ghodousi, J., & Ahmadi, H. (2010). SWAT-simulated hydrological impact of land-use change in the Zanjanrood Basin, Northwest Iran. *Hydrological Processes, 24*(7), 892–903.

Ghobadi, Y., Pradhan, B., Shafri, H., & Kabiri, K. (2015). Assessment of spatial relationship between land surface temperature and landuse/cover retrieval from multi-temporal remote sensing data in South Karkheh Sub-basin, Iran. *Arabian Journal of Geosciences, 8*(1), 525–537.

Gonzalez, P. (2001). Desertification and a shift of forest species in the West African Sahel. *Climate Research, 17*, 217–228.

Grunblatt, J., Ottichilo, W. K., & Sinange, R. K. (1992). A GIS approach to desertification assessment and mapping. *Journal of Arid Environments, 23*, 81–102.

Higuchi, A., Hiyama, T., Fukuta, Y., Suzuki, R., & Fukushima, Y. (2007). The behaviour of a surface temperature/vegetation index (TVX) matrix derived from 10-day composite AVHRR images over monsoon Asia. *Hydrological Processes, 21*, 1157–1166.

Huete, A. R., Jackson, R. D., & Post, D. F. (1985). Spectral response of a plant canopy with different soil backgrounds. *Remote Sensing of Environment, 17*, 37–53.

Indoitu, R., Kozhoridze, G., Batyrbaeva, M., Vitkovskaya, I., Orlovsky, N., Blumberg, D., et al. (2015). Dust emission and environmental changes in the dried bottom of the Aral Sea. *Aeolian Research, 17*, 101–115.

Jafari, R., & Bakhshandehmehr, L. (2013). Quantitative mapping and assessment of environmentally sensitive areas to desertification in central iran. *Land Degradation and Development*. doi:10.1002/ldr.2227.

Jury, M. R., Weeks, S., & Godwe, M. P. (1997). Satellite-observed vegetation as an indicator of climate variability over southern Africa. *South African Journal of Science, 93*, 34–38.

Karimkoshteh, M. H., & Haghiri, M. (2004). Water-reform strategies in Iran's agricultural sector. *Perspectives on Global Development and Technology, 3*(3), 327–346.

Kellogg, C. H., & Zhou, X. (2014). Impact of the construction of a large dam on riparian vegetation cover at different elevation zones as observed from remotely sensed data. *International Journal of Applied Earth Observation and Geoinformation, 32*, 19–34.

Khodagholi, M., Sabouhi, R., & Skandari, Z. (2014). Analysing past and future drought in Isfahan province. *Journal of Water and Soil Sciences, 67*, 367–379.

Kiage, L. M., Liu, K. B., Walker, N. D., Lam, N., & Huh, O. K. (2007). Recent land cover/use change associated with land degradation in the Lake Baringo catchment, Kenya, East Africa: evidence from Landsat TM and ETM+. *International Journal of Remote Sensing, 28*(19), 4285–4393.

König, H. J., Zhen, L., Helming, K., Uthes, S., Yang, L., Cao, X., et al. (2014). Assessing the impact of the sloping land conversion programme (SLCP) on rural sustainability in Guyuan, Western China. *Land Degradation & Development, 25*(4), 385–396.

Landis, J. R., & Koch, G. G. (1977). The measurement of observer agreement for categorical data. *Biometrics, 33*, 159–174.

Le Houérou, H. N. (Ed.). (1992). *An overview of vegetation and land degradation in world arid lands* (Vol. pp. 127e163). Texas: Texas Tech University.

Lieskovský, J., & Kenderessy, P. (2014). Modelling the effects of vegetation cover and different tillage practices on soil erosion in vineyards: a case study in Vrable (Slovakia) using WATEM/SEDEM. *Land Degradation & Development, 25*(3), 288–296.

Lillesand, T. M., & Kiefer, R. W. (2000). *Remote sensing and image interpretation*. New York: Wiley.

Liu, L., & Zhang, Y. (2011). Urban heat island analysis using the Landsat TM data and ASTER data: a case study in Hong Kong. *Remote Sensing, 3*, 1535–1552.

Liu, Z., Yao, Z., Huang, H., Wu, S., & Liu, G. (2014). Land use and climate changes and their impacts on runoff in the Yarlung Zangbo Basin, China. *Land Degradation & Development, 25*(3), 203–215.

Lyon, J. G., & Greene, R. G. (1992). Use of aerial photographs to measure the historical areal extent of Lake Erie coastal wetlands. *Photogrammetric Engineering and Remote Sensing, 58*(9), 1355–1360.

Mas, J. F. (1999). Monitoring land-cover changes: a comparison of change detection techniques. *International Journal of Remote Sensing, 20*(1), 139–152.

Matkan, A. H., Shakiba, A. R., & Hosseiniasl, A. (2010). Analysing the effect of Taleghan Dam on land cover changes. *Applied Research Journal of Geographic sciences, 116*(19), 45–64.

Mekonnen, M., Keesstra, S. D., Stroosnijder, L., Baartman, J., & Maroulis, J. (2015). Soil conservation through sediment trapping: a review. *Land Degradation & Development, 26*, 544–556.

Miao, L., Moore, J. C., Zeng, F., Lei, J., Ding, J., He, B., et al. (2015). Footprint of research in desertification management in China. *Land Degradation & Development, 26*, 450–457.

Micklin, F. (2007). The Aral Sea disaster. *Annual Review of Earth and Planetary Sciences, 35*, 47–72.

Modarres, R., Paulo, V., & Silvab, R. (2007). Rainfall trends in arid and semi-arid regions of Iran. *Journal of Arid Environments, 70*, 344–355.

Molle, F., & Mamanpoush, A. R. (2002). The 1999–2001 drought in the Zayandeh Rud basin and its impact on water allocation and agriculture. Report, Agricultural Research and Education Organization, Isfahan, Iran.

Momeni, M., & Saradjian, M. (2008). A weighted least squares approach for estimation of land surface temperature using constraint equations. *Photogrammetric Engineering and Remote Sensing, 74*(5), 637–646.

Moreno-Ramón, H., Quizembe, S. J., & Ibáñez-Asensio, S. (2014). Coffee husk mulch on soil erosion and runoff: experiences under rainfall simulation experiment. *Solid Earth, 5*(2), 851–862. doi:10.5194/se-5-851-2014.

Mundia, C. N., & Aniya, M. (2006). Dynamics of landuse/cover changes and degradation of Nairobi City, Kenya. *Land Degradation and Development, 17*(1), 97–108.

Myneni, R., Keeling, C. D., Tucker, C. J., Asrar, G., & Nemani, R. R. (1997). Increased plant growth in northern high latitudes from 1981 to 1991. *Nature, 386*, 698–702.

Najafi, A., & Vatanfada, J. (2011). Environmental challenges in trans-boundary waters, case study: Hamoon Hirmand Wetland (Iran and Afghanistan). *International Journal of Water Resources and Arid Environments, 1*(1), 16–24.

NDWMC (2015). I.R.of IRAN Meteorological Organization. National Drought Warning and Monitoring Centre, Drought Mapping at National Scale. http://ndwmc.irimo.ir/far/.Accessed. Accessed 25 Apr 2015.

Nicholson, S. E., Tucker, C. J., & Ba, M. B. (1998). Desertification, drought, and surface vegetation: an example from the West African Sahel. *Bulletin of the American Meteorological Society, 79*, 1–15.

Nourian, M. (2014). Detection of drought effects on land cover changes using meteorological and remote sensing data in the west of Isfahan province. Dissertation, Isfahan University of Technology.

Palmeirim, A. F., Peres, C. A., & Rosas, F. C. W. (2014). Giant otter population responses to habitat expansion and degradation induced by a mega hydroelectric dam. *Biological Conservation, 174*, 30–38.

Plesník, J. (2011). A concept of a degraded ecosystem in theory and practice—a review, The European Topic Centre on Biological Diversity (ETC/BD).

Price, J. C. (1990). The potential of remotely sensed thermal infrared data to infer surface soil moisture and evaporation. *Water Resources, 16*, 787–795.

Prince, S. D. (1991). Satellite remote sensing of primary production: comparison of results for Sahelian grasslands 1981-1988. *International Journal of Remote Sensing, 12*, 1301–1311.

Prince, S. D., & Justice, C. O. (1991). Coarse resolution remote sensing in the Sahelian environment. *International Journal of Remote Sensing, 12*, 1133–1421.

Prince, S. D., Brown de Colstoun, E., & Kravitz, L. (1998). Evidence from rain use efficiencies does not support extensive Sahelian desertification. *Global Change Biology, 4*, 359–374.

Rautela, P., Rakshit, R., Rajesh, V. K. J., Gupta, K., & Munshi, A. (2002). GIS and remote sensing-based study of the reservoir-induced land-use/land-cover changes in the catchment of Tehri dam in Garhwal Himalaya, India. *Current Science Journal, 83*(3), 308–311.

Ravi, S., Breshears, D. D., Huxman, T. E., & D'Odorico, P. (2010). Land degradation in drylands: interactions among hydrologic-aeolian erosion and vegetation dynamics. *Geomorphology, 116*, 236–245.

Requier Desjardins, M., Adhikari, B., & Sperlich, S. (2011). Some notes on the economic assessment of land degradation. *Land Degradation & Development, 22*, 285–298.

Sabzalipour, A. A., Seif, Z., & Qiyami, F. (2013). Temperature trend analysis in arid and semi-arid lands of Iran. *Geography and Development Iranian Journal, 30*, 117–138.

Sadeghi, S. H. R., Gholami, L., Sharifi, E., Khaledi Darvishan, A., & Homaee, M. (2015). Scale effect on runoff and soil loss control using rice straw mulch under laboratory conditions. *Solid Earth, 6*(1), 1–8.

Salazar, A., Baldi, G., Hirota, M., Syktus, J., & McAlpine, C. (2015). Land use and land cover change impacts on the regional climate of non-Amazonian South America: a review. *Global and Planetary Change, 128*, 103–119.

Serafini, V. V. (1987). Estimation of the evapotranspiration using surface and satellite data. *International Journal of Remote Sensing, 8*, 1547–1562.

Singh, A. (1989). Review article: digital change detection techniques using remotely-sensed data. *International Journal of Remote Sensing, 10*(6), 989–1003.

Smith, M. O., Ustin, S. L., Adams, J. B., & Gillespie, A. R. (1990). Vegetation in deserts: I. A regional measure of abundance from multispectral images. *Remote Sensing of Environment, 31*, 1–26.

Torres, L., Abraham, E. M., Rubio, C., Barbero-Sierra, C., & Ruiz-Pérez, M. (2015). Desertification research in Argentina. *Land Degradation & Development, 26*(5), 433–440.

Torres-Vera, M. A., Prol-Ledesma, R. M., & Garcia-Lopez, D. (2009). Three decades of land use variations in Mexico City. *International Journal of Remote Sensing, 30*(1), 117–138.

Tucker, C. J., Dregne, H. E., & Newcomb, W. W. (1991a). Expansion and contraction of the Sahara desert from 1980 to 1990. *Science, 253*, 299–301.

Tucker, C. J., Newcomb, W. W., Los, S. O., & Prince, S. D. (1991b). Mean and inter-annual variation of growing-season normalized difference vegetation index for the Sahel 1981-1989. *International Journal of Remote Sensing, 12*, 1133–1135.

USGS (2013). United States Geological Survey. Using the USGS Landsat 8 Product. http://landsat.usgs.gov/Landsat8_Using_Product.php. Accessed 25 Apr 2015.

Vandandorj, S., Gantsetseg, B., & Boldgiv, B. (2015). Spatial and temporal variability in vegetation cover of Mongolia and its implications. *Journal of Arid Land, 7*(4).

Vieira, R. M. S. P., Tomasella, J., Alvalá, R. C. S., Sestini, M. F., Affonso, A. G., Rodriguez, D. A., et al. (2015). Identifying areas susceptible to desertification in the Brazilian northeast. *Solid Earth, 6*(1), 347–360.

Wijesundara, C. J., & Dayawansa, N. D. K. (2011). Construction of large dams and their impact on cultural landscape: a study

in Victoria reservoir and the surrounding area. *Tropical Agricultural Research, 22*(2), 211–219.

WRM (2015). Iran Water Resources Management Company (WRM), Statistices on Dam Projects. http://daminfo.wrm.ir/fa/dam/stats. Accessed 31 May 2015.

Xiao, H., & Weng, Q. (2007). The impact of land use and land cover changes on land surface temperature in a karst area of China. *Journal of Environmental Management, 85*(1), 245–257.

Xie, L. W., Zhong, J., Chen, F. F., Cao, F. X., Li, J. J., & Wu, L. C. (2015). Evaluation of soil fertility in the succession of karst rocky desertification using principal component analysis. *Solid Earth, 6*(2), 515–524.

Zafarnejad, F. (2009). The contribution of dams to Iran's desertification. *International Journal of Environmental Studies, 66*(3), 327–341.

Zhang, W., He, Y., Cai, J., & Li, Z. (2010). GIS-based analysis on the relationship between land use/cover and land surface temperature in Zhejiang Province. *Chinese Journal of Agrometeorology, 10*, 295–299.

Zhang, J., Niu, J. M., Bao, T., Buyantuyev, A., Zhang, Q., Dong, J. J., et al. (2014). Human induced dryland degradation in Ordos Plateau, China, revealed by multilevel statistical modeling of normalized difference vegetation index and rainfall time-series. *Journal of Arid Land, 6*(2), 219–229.

Zhao, G., Mu, X., Wen, Z., Wang, F., & Gao, P. (2013). Soil erosion, conservation, and eco-environment changes in the loess plateau of China. *Land Degradation & Development, 24*, 499–510.